Dynamics of Simultaneous Ordering and Phase Separation and Effect of Long-Range Coulomb Interactions

L. Q. Chen
Department of Materials Science and Engineering, Pennsylvania State University, University Park, Pennsylvania 16802

A. G. Khachaturyan
Department of Materials Science and Engineering, P.O. Box 909, Rutgers University, Piscataway, New Jersey 08855-0909
(Received 18 November 1992)

The dynamics of simultaneous ordering and phase separation in the presence of a long-range Coulomb interaction is investigated by a computer simulation. It is shown that an intermediate nonstoichiometric ordered single phase appears as a transient phase during decomposition of a binary homogeneous disordered solid solution into an equilibrium two-phase mixture of ordered and disordered phases. Introduction of the long-range Coulomb interactions results in a mesoscale phase which consists of periodical arrays of ordered phase particles embedded in a disordered matrix.

PACS numbers: 64.70.Kb, 81.30.Mh, 82.20.Wt

Simultaneous ordering and phase separation is a very common and complex phenomenon in metallic alloys, ceramics, and minerals and even compound semiconductors. It occurs during decomposition of a homogeneous disordered phase into a two-phase mixture of ordered and disordered phases. Its dynamics has been explored recently by various techniques including computer simulations [1–3], thermodynamic stability analyses [4–6], and experiments [7–10]. However, the effect of long-range Coulomb interaction on the nonlinear dynamics of ordering and phase separation seems to have never been discussed, although it is directly related to the interesting phenomenon of nanoscale ordered domain formation in oxide compounds, $A(B'_{1/3}B''_{2/3})O_3$, where A, B', and B'' are cations with different valences.

Virtually all previous theories of diffusional phase transformations are based on the finite-range model of interatomic interactions. This is the main reason why the total configurational energy of a multiphase system can be presented as a sum of the bulk and interfacial energies. The interfacial energy, unlike the bulk energy, depends on the multiphase morphological pattern. However, if the interatomic interaction radius is infinite (or very long), a separation of the total configuration energy into the bulk and interfacial energies becomes problematic. In such a case, not only the interfacial energy but also the bulk energy itself become functions of the multiphase mesoscale structural pattern. Familiar examples are ferromagnetics, ferroelectrics, and coherent multiphase mixtures characterized by the infinite-range magnetic, electric, and elastic dipole-dipole interactions which control their mesoscale morphologies.

Ceramic compounds are typical examples of systems with another type of long-range interatomic interaction, the Coulomb interaction. A model system which will be considered below is a ceramic compound undergoing a diffusional transformation involving ions of the same sign, say, cations, whereas the diffusion of ions of opposite sign, anions occupying different sublattices, are practically frozen. We assume that the finite-range interaction alone would result in decomposition of a disordered phase into a mixture of ordered and disordered phases. The question is how the kinetics of decomposition will be affected by the introduction of a long-range Coulomb interaction. It is qualitatively clear that the presence of a long-range Coulomb interaction requires that the phase separation occurs at a larger undercooling since any clustering of ions of the same charge results in a local charge inhomogeneity which generates local electric fields. This violation of the local charge neutrality should dramatically increase the electrostatic energy of a system, the larger the increase, the larger being the scale of the charge inhomogeneities. We may expect that a balance between the finite-range interaction and the long-range Coulomb interaction produces a stable inhomogeneous mesoscopic state.

The idea that long-range Coulomb interaction may result in the formation of stable charge density waves was suggested and analyzed in the framework of the linearized Cahn-Hilliard kinetic equation by Cahn and Gupta [11]. It has been also recently suggested [12] that the long-range Coulomb and elastic interactions might be responsible for the formation of nanoscale structural states [13].

In this paper, we will investigate the nonlinear dynamics of morphological evolution by employing a computer simulation technique which we recently proposed [1]. It is based on the numerical solution of the nonlinear Onsager equations for microscopic atomic diffusion with respect to occupation probabilities, $n(\mathbf{r},t)$, to find one kind of cation at the cation sublattice site $\mathbf{r}$ at the time t [14]. This equation reads

$$\frac{dn(\mathbf{r},t)}{dt}=\sum_{\mathbf{r}'}L(\mathbf{r}-\mathbf{r}')\frac{\delta F}{\delta n(\mathbf{r}',t)}\,, \tag{1}$$

where $L(\mathbf{r}-\mathbf{r}')$ are the kinetic coefficients proportional to

the probabilities of elementary diffusional jumps from site $\mathbf{r}$ to $\mathbf{r}'$ during the time unit and F is the free energy depending on both the long-range and finite-range interactions. The summation in (1) is carried out over all cation sublattice sites of a system. In the long-wave limit, Eq. (1) is reduced to the nonlinear Cahn-Hilliard equation. For the free energy, we employ the mean-field approximation [1]. This approximation does not introduce any substantial error since mesoscopic phases, if they appear, are associated with the long-wave asymptotic of the free energy which can be reduced to the conventional Landau free energy expansion with the gradient energy term, plus the substantially nonlocal singular term associated with the Coulomb interaction. Employing a more accurate free energy model just changes the Landau expansion coefficient and, thus, may affect only the scale of the mesoscopic structure. This physical interpretation is substantiated by the recent work of Roland and Desai [15] who demonstrated, in their 2D computer simulation study of an ordering system, that it is this singularity at $\mathbf{k}=0$ in the k-space representation of the Landau free energy expansion which results in the stable mesoscopic state.

To demonstrate the dynamics of the formation of mesoscopic states, we employ a two-dimensional (2D) model with a square lattice. An atomic interaction with a finite-range part which favors decomposition of a homogeneous disordered phase into a mixture of ordered and disordered phases together with a long-range screened Coulomb interaction is assumed. The finite-range interaction $W(\mathbf{r}-\mathbf{r}')_{\text{fi}}$ is, particularly, described by a set of values:

$$W_1=1.0\,\text{eV},\quad W_2=-0.8\,\text{eV},\quad W_3=-0.55\,\text{eV}, \tag{2}$$

where W_1, W_2, and W_3 are first-, second-, and third-nearest-neighbor interchange energies defined by $W(r)=V_{AA}(r)+V_{BB}(r)-2V_{AB}(r)$ with $V_{AA}(r)$, $V_{BB}(r)$, and $V_{AB}(r)$ the pairwise interaction energies of A-A, B-B, and A-B pairs of atoms placed at the sites separated by a distance r. The number of nearest neighbors and the value of the interchange energies in the finite-range interaction model are quite arbitrarily chosen with only one requirement that they produce a two-phase field of ordered and disordered phases. The Fourier transform of this finite-range interaction is

$$V(\mathbf{k})_{\text{fi}}=2W_1[\cos 2\pi h+\cos 2\pi l]+4W_2\cos 2\pi h\cos 2\pi l +2W_3[\cos 4\pi h+\cos 4\pi l], \tag{3}$$

where h and l are related to the reciprocal lattice vector $\mathbf{k}$ by $\mathbf{k}=(2\pi/a_0)(h,l)$ in which a_0 is the lattice parameter of the square lattice. Since the minimum of $V(\mathbf{k})$ falls at $\mathbf{k}_0=(2\pi/a_0)(\frac{1}{2},\frac{1}{2})$, this finite-range interaction alone would result in the precipitation of an ordered phase at low temperatures characterized by the $(\frac{1}{2},\frac{1}{2})$ superlattice diffraction maximum. The mean-field phase diagram calculated using this finite-range interaction model is presented in Fig. 1. The diagram shows the ordering

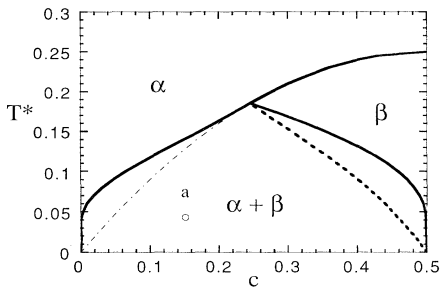

FIG. 1. Equilibrium phase diagram calculated using the finite-range interaction model with parameters given in (2). α represents the disordered phase and β the ordered phase. The thick lines are phase boundaries. The dot-dashed line is the ordering instability line which coincides with the left branch of the spinodal line of the ordered phase. The dotted line is the other branch of spinodal line of the ordered phase.

transition line of the second kind terminated by the tricritical point at $c=0.255$ and $T^*=0.19$ below which there is a two-phase field describing equilibrium between a disordered phase and an ordered phase. In the phase diagram, T^* is a reduced temperature equal to $k_BT/|V(\mathbf{k}_0)|$.

The finite-range interaction (2) is competed by a screened Coulomb repulsion given by

$$W(\mathbf{r})_{\text{Coul}}=\frac{A}{r}\exp\left(-\frac{r}{r_D}\right), \tag{4}$$

where r_D is the screening radius, r is the distance, and A is a parameter which measures the strength of the long-range Coulomb interaction. The long-wave asymptote of the Fourier transform of (3) is $V(\mathbf{k})_{\text{fi}}\approx V(0)_{\text{fi}}+\mu k^2+\cdots$, while the asymptote for (4) is $V(\mathbf{k})_{\text{Coul}}\approx 4\pi A/v_0(k^2+k_D^2)$ [k_D is $2\pi/r_D$, v_0 is the atomic volume, and $V(\mathbf{k})_{\text{Coul}}$ is singular at $k=0$ for $r_D\rightarrow\infty$].

Numerical solution to the nonlinear equation (1) was obtained using its Fourier representation where the long-range Coulomb interaction can be easily incorporated. The solutions, the Fourier components $\tilde{n}(\mathbf{k},t)$ of the occupation probabilities, are then transformed back to $n(\mathbf{r},t)$ to produce the temporal evolution of the atomic structure and mesoscale morphologies. The reciprocal space formulation automatically implies the application of periodic boundary conditions.

An example of the structural transformation sequence from a disordered phase to a mesoscopic one is shown in Fig. 2. It was obtained by "isothermal aging" of a completely disordered state of composition 0.175 at a reduced temperature $T^*=0.0426$. The corresponding point is shown in Fig. 1 by the letter "a." A small random noise is provided at the very beginning of the simulation. The parameter A is chosen to be 0.25 eV and the screening length is $10a_0$. The computational supercell consists of 128×128 square unit cells. It is shown in Fig. 2 that the first state of phase transformation is a congruent ordering

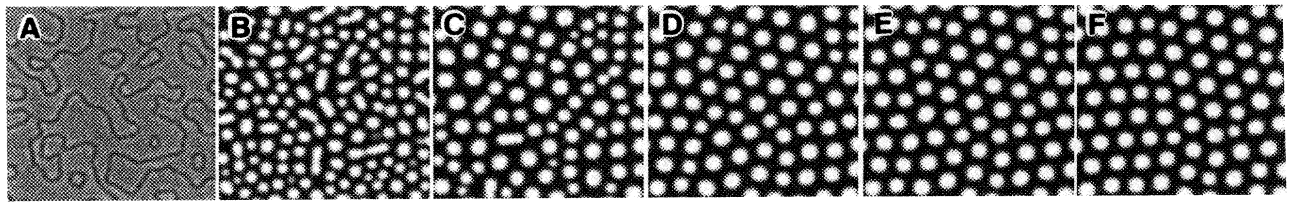

FIG. 2. Temporal morphological evolution started from a completely disordered state with $A=0.25$ eV and composition $c=0.175$. The gray level represents the different magnitudes of the absolute value of $c\eta$, where c is the local composition and η is the local long-range order parameter of the ordered phase; c and η are related to the occupation probability by $n(\mathbf{r})=c(\mathbf{r})+c(\mathbf{r})\eta(\mathbf{r})$. In this representation, bright regions are ordered domains and dark regions are disordered phase domains. (a) $t^*=2.5$; (b) $t^*=10$; (c) $t^*=100$; (d) $t^*=500$; (e) $t^*=1000$; (f) $t^*=2000$.

which produces an intermediate nonstoichiometric ordered single-phase state consisting of antiphase domains [Fig. 2(a)]. This intermediate phase has approximately the same composition as the original disordered phase throughout the system except in regions close to the antiphase domain boundaries (APBs). Later the intermediate ordered state decomposes starting from the APBs which are replaced by layers of the equilibrium disordered phase [Fig. 2(b)]. This is the interesting kinetic process which we recently predicted for precipitation of an ordered intermetallic phase from a disordered matrix [1]. The new feature induced by the long-range Coulomb interaction is a dramatic change in the decomposition of the intermediate ordered phase and the subsequent coarsening process. In systems with only finite-range interactions, the resultant two-phase mixture will continuously coarsen reducing its interfacial energy. Our computer simulation demonstrates that the Coulomb interaction stops the coarsening after the ordered particles reach a certain size. Eventually, all ordered particles reach the same size and form a spectacular regular pattern of a triangular lattice [Fig. 2(f)]. Figure 3 shows the corresponding atomic structures of the starting state [Fig. 3(a)], the intermediate single-phase ordered state [Fig. 3(b)], and the final mesoscopic state [Fig. 3(c)]. Figures 3(b) and 3(c) correspond to the 32×32 unit cells in the lower-left corner of Figs. 2(a) and 2(f).

Our simulation also demonstrates that changing electrostatic potentials (4) just affects the size of ordered particles and the distance between them. It is illustrated by a comparison between Figs. 4(a) and 4(b). If the average composition increases, an interconnected morphology [Fig. 5(a)] or isolated disordered particles (dark) in the ordered matrix (bright) [Fig. 5(b)] is observed.

The typical scale of the mesoscale phase can be estimated by using the Ginzburg-Landau phenomenological free energy model [11]. The gradient energy term in the phenomenological free energy model is $\sum_{\mathbf{k}}\frac{1}{2}\mu k^2|\tilde{c}(\mathbf{k})|^2$, where μ is the gradient energy coefficient, $\mathbf{k}$ is the wave vector of a concentration wave, and $\tilde{c}(\mathbf{k})$ is the Fourier transform of the concentration heterogeneities, $c(\mathbf{r})-\bar{c}$, where $c(\mathbf{r})$ is local composition and $\bar{c}$ is the average composition. The contribution of the long-range screened Coulomb interaction is $\frac{1}{2}\sum_{\mathbf{k}}[\gamma/(k^2+k_D^2)]|\tilde{c}(\mathbf{k})|^2$. Minimizing the sum

$$\phi(k)=\frac{\gamma}{k^2+k_D^2}+\mu k^2 \tag{5}$$

with respect to k, we obtain the minimum of $\phi(k)$ at $k_1=[(\gamma/\mu)^{1/2}-k_D^2]^{1/2}$. If $(\gamma/\mu)^{1/2}>k_D^2$ $[=(2\pi/r_D)^2]$, i.e., if the screening radius r_D is substantially greater than the correlation length $r_c=2\pi(\mu/\gamma)^{1/4}$, k_1 is a real positive number and the typical scale for a stable mesoscale phase will be $2\pi/k_1$.

The microscopic representation of the phenomenological coefficients γ and μ are given by

$$\gamma=\frac{4\pi A}{v_0},\quad \mu=\frac{1}{2}\left[\frac{\partial^2}{\partial\mathbf{k}^2}[V(\mathbf{k})+V(\mathbf{k}-\mathbf{k}_0)]\right]_{\mathbf{k}=0},$$

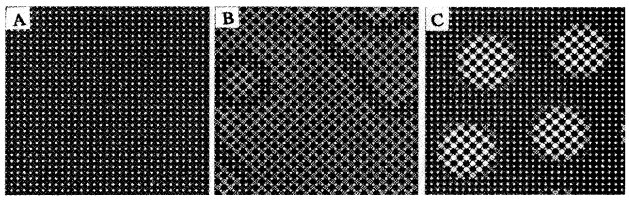

FIG. 3. The atomic structures (32×32) represented by the occupation probabilities taken from the lower-left corner of the pictures in Fig. 2. (a) The initial state, $t^*=0.0$; (b) $t^*=2.5$, the intermediate single-phase ordered state; and (c) $t^*=2000$, the mesoscopic state. Completely dark circle indicates the occupation probability $n(\mathbf{r})$ is 0.0 and completely bright is 1.0.

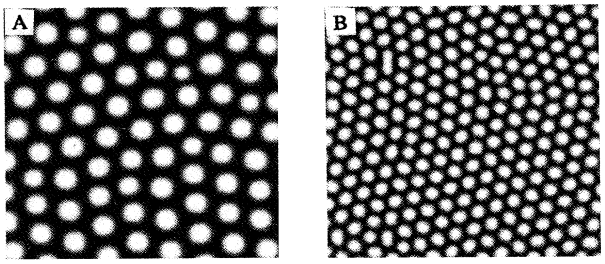

FIG. 4. The influence of the constant A on the size of ordered domains. The representation is the same as in Fig. 2. (a) $A=0.25$ eV, $t^*=2000$; (b) $A=1.0$ eV, $t^*=1000$.

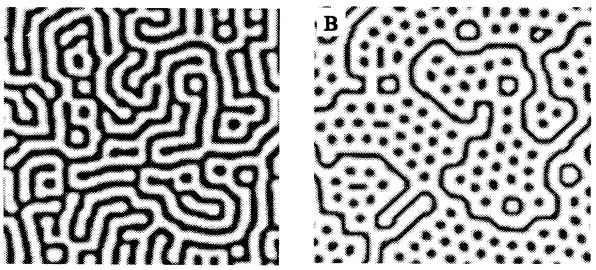

FIG. 5. The influence of average composition on the morphology of the mesoscale phase. The representation is the same as in Fig. 2. (a) $c=0.25$; (b) $c=0.33$. Compare them with Fig. 2(f).

where $\mathbf{k}_0$ is the wave vector of the primary $(\frac{1}{2},\frac{1}{2})$ ordering, A is the constant in (4), and v_0 is the unit cell volume. The characteristics of the function $\phi(k)$ calculated with the chosen parameters (2) are shown in Fig. 6. It reveals an important consequence of the long-range Coulomb contribution, a shift of the $\min\phi(k)$ position from the reciprocal lattice position $k=0$ to a nonzero one. If A is zero, $\min\phi(k)$ is at $k=0$ and, thus, the decomposition of the intermediate ordered phase is a normal spinodal decomposition which would lead to the conventional formation of two-phase mixture of ordered and disordered phases followed by normal coarsening. However, at finite values of A, the k for which ϕ is a minimum is finite and a mesoscopic phase will be formed with the scale $\lambda\sim k^{-1}$.

The predictions following from our simulation may have important implications to certain ceramic ionic materials. It is particularly attractive to assume that the nanoscale ordered domain formation in relaxor ferroelectric, $PbMg_{1/3}Nb_{2/3}O_3$ (PMN), as revealed in transmission electron microscopy [16–18], could be explained by the electrostatic interaction, as is suggested in [12,13, 16–18]. In PMN, nanoscale ordered domains are formed in a disordered matrix and those domains do not grow during prolonged aging, which contradicts all existing paradigms of normal coarsening kinetics. These unusual kinetic features, however, are successfully predicted by our computer simulation. Since the ordered domains in PMN are so small that the screening radius of the Coulomb interaction in this system is most likely longer than the typical ordered domain size, the electrostatic interaction between the ordered particles should play an important role. Formation of a mesoscopic phase should be actually a general phenomenon in ionic ceramics where the charge imbalance due to compositional segregation plays an important role.

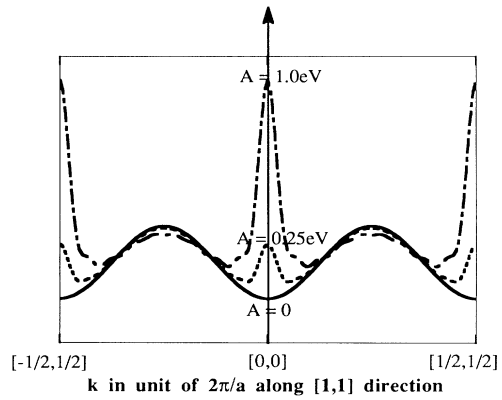

FIG. 6. The effect of different values of A on the function $\phi(k)$. $\phi(k)$ is plotted against k along the [1,1] direction for three different values of A.

L.Q.C. is partially supported by the Pennsylvania State University Faculty Research Fund and the computing time is provided by the Pittsburgh Supercomputing Center under Grant No. DMR900022P. A.K. is supported by National Science Foundation under Grant No. NSF-DMR-91-23167.

[1] L. Q. Chen and A. G. Khachaturyan, Scr. Metall. Mater. **25**, 61 (1991); Acta Metall. Mater. **39**, 2533 (1991).
[2] S. Matsumura, Y. Tanaka, K. Tanako, and K. Oki, in Proceedings of the International Workshop on Computational Materials Science, Tsukuba, Japan, 1990, pp. 231–234.
[3] K. Shiiyama, H. Kanemoto, H. Ninomiya, and T. Eguchi, in Proceedings of the International Workshop on Computational Materials Science, Tsukuba, Japan, 1990 (Ref. [2]), pp. 103–110.
[4] S. M. Allen and J. W. Cahn, Acta Metall. **24**, 425 (1976).
[5] A. G. Khachaturyan, T. F. Lindsey, and J. W. Morris, Jr., Met. Trans. **19A**, 249 (1988).
[6] W. A. Soffa and D. E. Laughlin, Acta Metall. **37**, 3019 (1989).
[7] C. L. Corey, B. Z. Rosenblum, and G. M. Greene, Acta Metall. **21**, 837 (1973).
[8] T. Sato, N. Tanaka, and T. Takahashi, Trans. Jpn. Inst. Met. **29**, 17 (1988).
[9] M. Radmilovich, A. G. Fox, and G. Thomas, Acta Metall. **37**, 2385 (1989).
[10] S. Matsumura, H. Oyama, and K. Oki, Mater. Trans. Jpn. Inst. Metals **30**, 695 (1989).
[11] J. W. Cahn (private communication); K. Gupta, Sc. D. thesis, MIT, 1976.
[12] D. Vieland, P. Lourdis Salamanca-Riba, and M. Wuttig, in *Kinetics of Ordering Transformations in Metals*, edited by H. Chen and V. Vasudevan (Minerals, Metals and Materials Society, Warrendale, PA, 1992), pp. 77–86.
[13] L. E. Cross, Ferroelectrics **76**, 241 (1987).
[14] A. G. Khachaturyan, *Theory of Structural Transformations in Solids* (Wiley, New York, 1983).
[15] C. Roland and R. C. Desai, Phys. Rev. B **42**, 6658 (1990).
[16] J. Chen, H. Chen, and M. A. Harmer, J. Am. Ceram. Soc. **72**, 593 (1989).
[17] E. Hussan, M. Chubb, and A. Morall, Mater. Res. Bull. **33**, 357 (1988).
[18] C. A. Randall and A. S. Bhalla, Jpn. J. Appl. Phys. **29**, 327 (1990).

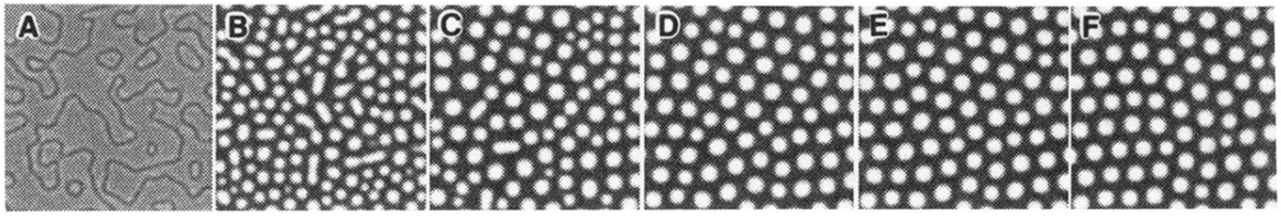

FIG. 2. Temporal morphological evolution started from a completely disordered state with $A=0.25$ eV and composition $c=0.175$. The gray level represents the different magnitudes of the absolute value of $c\eta$, where c is the local composition and η is the local long-range order parameter of the ordered phase; c and η are related to the occupation probability by $n(\mathbf{r})=c(\mathbf{r})+c(\mathbf{r})\eta(\mathbf{r})$. In this representation, bright regions are ordered domains and dark regions are disordered phase domains. (a) $t^*=2.5$; (b) $t^*=10$; (c) $t^*=100$; (d) $t^*=500$; (e) $t^*=1000$; (f) $t^*=2000$.

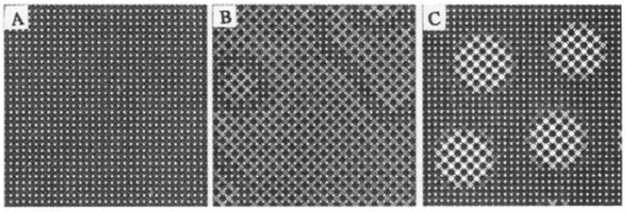

FIG. 3. The atomic structures (32×32) represented by the occupation probabilities taken from the lower-left corner of the pictures in Fig. 2. (a) The initial state, $t^*=0.0$; (b) $t^*=2.5$, the intermediate single-phase ordered state; and (c) $t^*=2000$, the mesoscopic state. Completely dark circle indicates the occupation probability $n(\mathbf{r})$ is 0.0 and completely bright is 1.0.

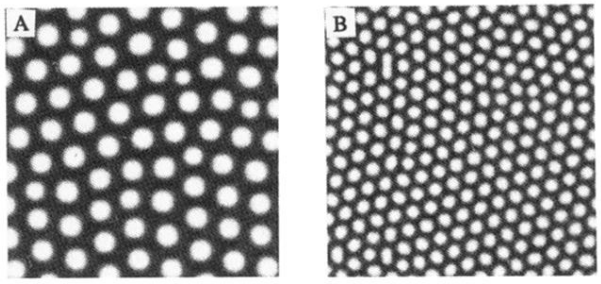

FIG. 4. The influence of the constant A on the size of ordered domains. The representation is the same as in Fig. 2. (a) $A = 0.25$ eV, $t^* = 2000$; (b) $A = 1.0$ eV, $t^* = 1000$.